

Electronic Supplementary Information

Chemical Design Homochiral Heterocyclic Organic Ferroelectric Crystals

Xian-Jiang Song,^a Shu-Yu Tang,^a Xiao-Gang Chen,^a Yong Ai*

Experimental Part

Materials. Camphor, (-)-(camphorylsulfonyl)imine, Selenium dioxide, Acetic Acid, 3-Bromo-1-propanol, and 1,8-diazabicyclo[5.4.0]undec-7-ene (DBU) were purchased from Energy Chemical, Leyan company and used as-received. Dichloromethane (DCM) and toluene were purchased from Merck and used as the solvent.

Vibrational circular dichroism (VCD) and Infrared (IR) measurement. The VCD and IR measurements were both carried out by using a Bruker PMA-50 instrument, and they are tested separately by selecting the parameters corresponding to VCD and IR. At room temperature, the humidity of the desiccant in the instrument does not exceed 20%, and it is protected by nitrogen purging. Moreover, an appropriate amount of liquid nitrogen should be added to provide a low temperature working environment for the detector. The sample needs to be mixed with KBr and ground into a powder, and then it should be pressed into a thin and transparent continuous sheet as much as possible.

Single-crystal diffraction. The variable temperature single crystal X-ray diffraction (XRD) data was carried out by using a Rigaku Oxford diffractometer with MoK α radiation ($\lambda = 0.71073 \text{ \AA}$). The test sample should be a high-quality single crystal that has just been precipitated. The direct method was used to solve the crystal structure at various temperatures, and the SHELXTL-2014 program package was used to correct it by the full matrix least squares method. For all non-hydrogen atoms, their anisotropy is refined. All hydrogen atoms are generated geometrically and at the same time in proper positions.

PXRD. Variable-temperature powder X-ray diffraction measurements were performed on a Rigaku

D/MAX 2000 PC X-ray diffractometer. The measurement condition is in a 2θ range of 5° – 50° , the step size is 0.02° , and the corresponding PXRD pattern is obtained.

Differential scanning calorimetry (DSC). The DSC measurement is performed by using a PerkinElmer Diamond DSC instrument. Added the powder sample to an alumina crucible and cover it. Then the powder sample was studied in by heating and cooling with a rate of 20 K min^{-1} at nitrogen atmosphere.

Second Harmonic Generation (SHG). The SHG measurements was carried on the FLS 920, Edinburgh Instruments and the laser of Vibrant 355 II, OPOTEK (wavelength 1064 nm, pulse Nd:YAG).

PFM measurements. The ferroelectric domain structures were performed on a commercial atomic force microscope system (MFP-3D, Asylum Research). Conductive Pt/Ir-coated silicon probes (EFM-50, Nanoworld) were used for domain imaging and polarization switching studies. Resonant-enhanced PFM mode was used to enhance the signal, with the ac voltage frequency of about 330-380 kHz. The as-grown thin films of 1-SSR or *l*-RRS on ITO-coated glass, was used for the PFM measurements. Specifically, 20 μL of ethanol solution of 1-SSR or *l*-RRS (20 mg per 200 μL) was dripped onto a $1\text{ cm} \times 1\text{ cm}$ ITO glass sheet, and the solvent was volatilized at room temperature to grow a smooth crystal film.

Polarization-Electric Field (*P-E*) Hysteresis Loops. *P-E* hysteresis loops measurements were recorded using the double-wave method at 298 K. The double-wave method was carried out with a homemade system, including high voltage amplifier (Trek 623B), waveform generator (Agilent 33521A), and low-current electrometer (Keithley 6514). The measuring frequency was 0.05 Hz. A crystal capacitor, made by a high-quality single crystal and a commercial IC six-hole socket, was fabricated for the *P-E* hysteresis loop measurement.

NMR spectroscopy. Dissolve a small amount of crystals in an appropriate amount of deuterated chloroform, and use the NMR spectrometer (Magnet system 300'54 Ascend ULH) produced by Bruker Switzerland AG to perform the NMR test. The working frequency of ^1H NMR is 300 MHz, the spectral width is 300 Hz, the test temperature is 298 K, the ambient humidity is 45 %, the acquisition time is 3 s, the number of scans is 16 times, and the excitation pulse is 1211 μs . Before processing the spectrum, perform phase correction and baseline leveling. All spectra are processed by Topspin 4.0.8 software.

Synthesis of (-)-(3-Oxocamphorylsulfonyl)imine. The synthesis of (-)-(3-Oxocamphorylsulfonyl)imine

was followed the reported recipe.¹ To a single-necked flask added 21.3 g (0.1 mol) (-)-(camphorylsulfonyl)imine, 15 g (0.135 mol) selenium dioxide, and 250 mL acetic acid as solvent. The reaction mixture was stirred and refluxed overnight. Then the mixture was filtered and black selenium was removed. The crude product was obtained after evaporator the acetic acid under vacuum. (-)-(3-oxocamphorylsulfonyl)imine was obtained as a yellow crystal through recrystallizing. ¹HNMR (300 MHz) δ 3.43 (d, J = 13.5 Hz, 1H), 3.22 (d, J = 13.5 Hz, 1H), 2.76 (d, J = 4.6 Hz, 1H), 2.43 - 2.21 (m, 2H), 2.09 - 1.91 (m, 1H), 1.87 - 1.71 (m, 2H), 1.17 (d, J = 10.2 Hz, 3H), 0.96 (d, J = 11.7 Hz, 3H).

Synthesis of (+)-(3-Oxocamphorylsulfonyl)imine. The same procedure was followed for the synthesis of (+)-(3-Oxocamphorylsulfonyl)imine. ¹HNMR (300 MHz, CDCl₃) δ 3.43 (d, J = 13.5 Hz, 1H), 3.22 (d, J = 13.5 Hz, 1H), 2.76 (d, J = 4.5 Hz, 1H), 2.39 - 2.16 (m, 2H), 2.08 - 1.89 (m, 1H), 1.82 (dd, J = 15.5, 5.6 Hz, 1H), 1.64 (s, 1H), 1.15 (s, 3H), 0.96 (d, J = 11.3 Hz, 3H).

Synthesis of 1-RRS. To a DCM solution containing (+)-10-Camphorsulfonylimine (7.00 g, 30.7 mmol) was added DBU (153 mmol, 5 equiv), and 2-bromoethanol (153 mmol, 5 equiv). The reaction mixture was stirred and refluxed for 3 h and then, was allowed to cool to room temperature. The reaction was washed with saturated aqueous NH₄Cl (2 \times 100 ml). the mixture was extracted with 3 \times 100 ml DCM. The organic layer was collected, dried over with MgSO₄, filtered, and concentrated. The crude product was washed with ethanol and dissolved in the methanol. White needle-like crystals of 1-RRS were obtained after 1 week. 72% yield, ee>99% [Daicel Chiralpak IA (4.6 mmI.D. * 250 mmL, 5 μ m), acetonitrile/*water* = 90/10, ν = 0.5 mL/min, λ = 320 nm, t = 6.98 min]. ¹HNMR (300 MHz) δ 4.50 (t, J = 12.4 Hz, 0H), 3.99 (dd, J = 11.6, 5.2 Hz, 0H), 3.86 - 3.56 (m, 1H), 3.33 (s, 1H), 2.54 - 2.21 (m, 1H), 2.13 - 1.92 (m, 0H), 1.89 - 1.70 (m, 1H), 1.34 (d, J = 13.6 Hz, 0H), 1.18 (s, 3H), 1.06 (s, 3H).

Synthesis of 1-SSR. The same procedure was followed for the synthesis of 1-SSR. 68% yield, ee>99% [Daicel Chiralpak IA (4.6 mmI.D. * 250 mmL, 5 μ m), acetonitrile/*water* = 90/10, ν = 0.5 mL/min, λ = 320 nm, t = 7.08 min]. ¹H NMR (300 MHz, CDCl₃) δ 4.49 (dd, J = 17.9, 6.8 Hz, 1H), 3.99 (dd, J = 11.5, 5.3 Hz, 1H), 3.85 - 3.58 (m, 2H), 3.33 (s, 2H), 2.52 - 2.17 (m, 3H), 2.01 (dt, J = 11.7, 10.5 Hz, 1H), 1.87 - 1.72 (m, 2H), 1.60 (s, 4H), 1.40 - 1.24 (m, 2H), 1.18 (s, 3H), 1.07 (s, 3H).

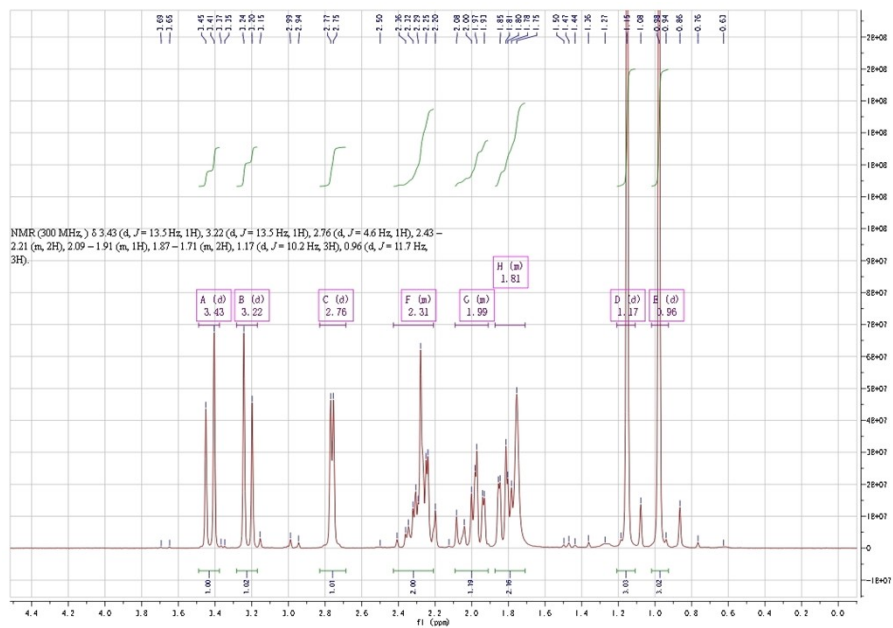


Fig. S1. Image of ^1H NMR (300 MHz) for (-)-(3-Oxocamphorylsulfonyl)imine.

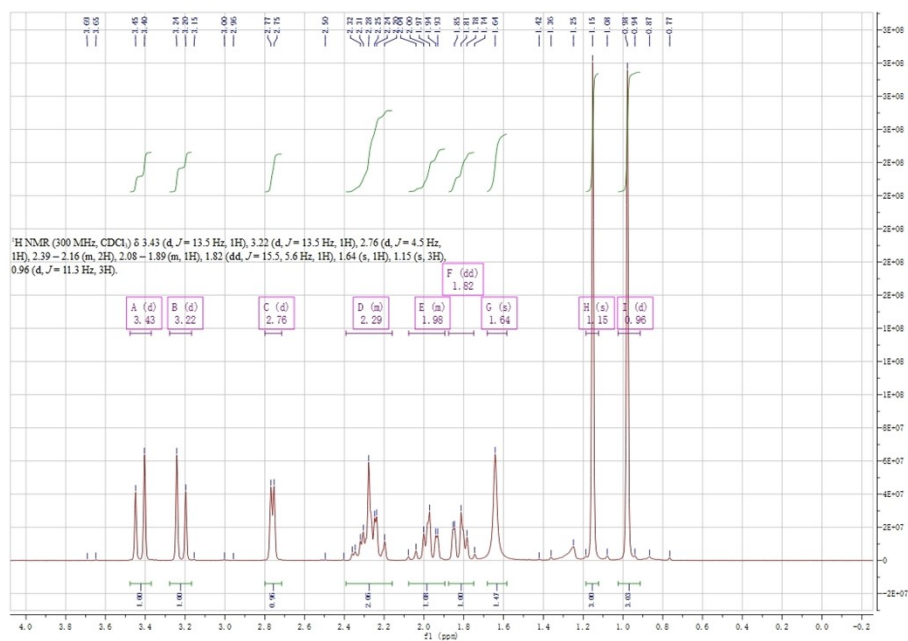


Fig. S2. Image of ^1H NMR (300 MHz) for (+)-(3-Oxocamphorylsulfonyl)imine.

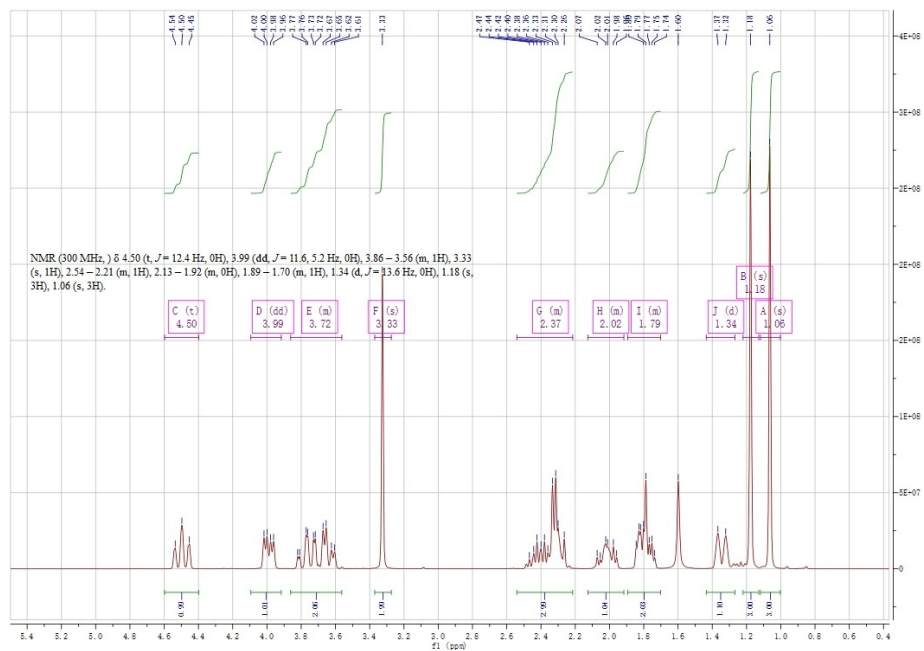


Fig. S3. Image of ^1H NMR (300 MHz) for 1-RRS.

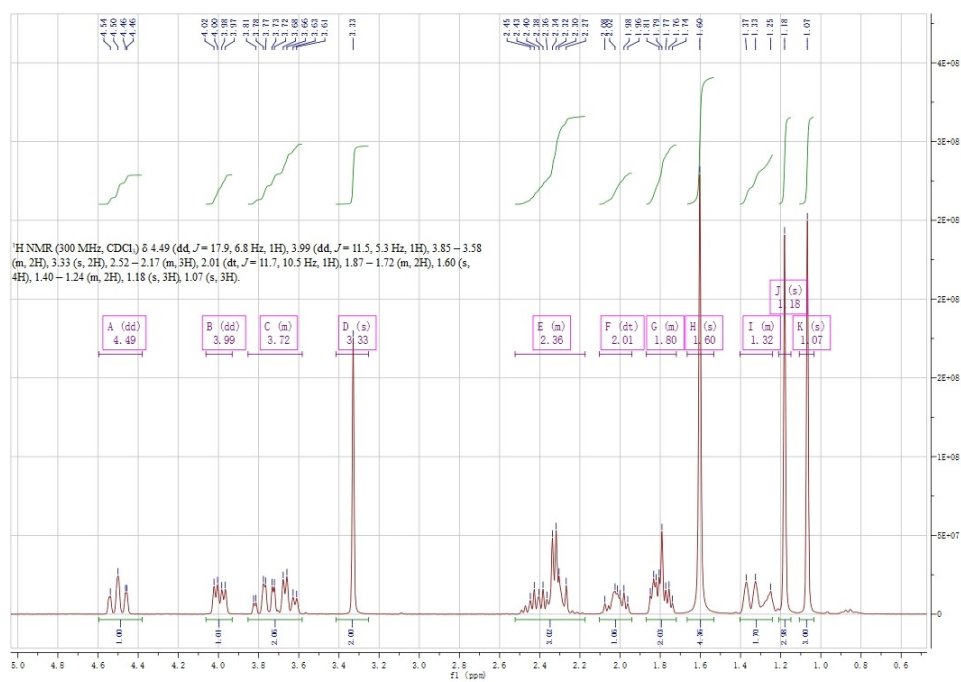


Fig. S4. Image of ^1H NMR (300 MHz) for 1-SSR.

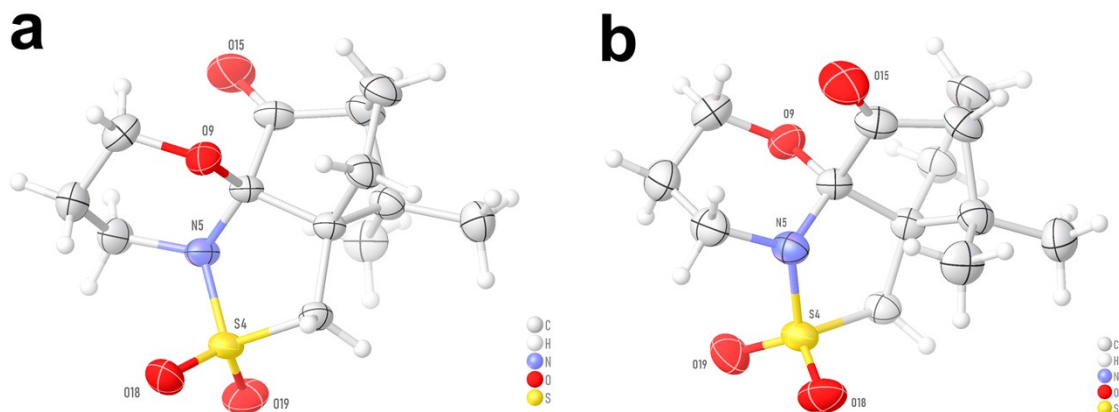


Fig. S5. The molecular structures of (a) 1-SSR and (b) 1-RRS with the atom. Displacement ellipsoids are drawn at the 50% probability level.

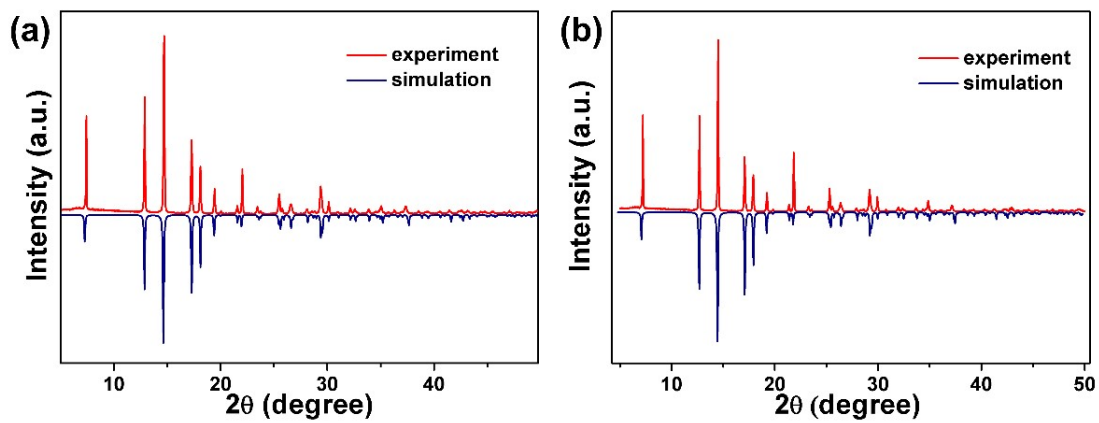


Fig. S6. Measured and simulated powder X-ray diffraction patterns of (a) 1-SSR and (b) 1-RRS.

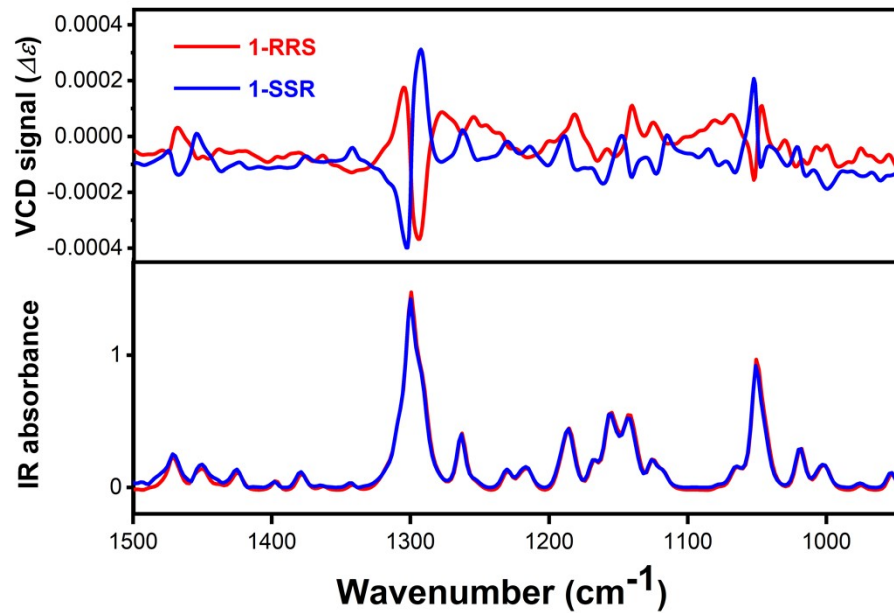


Fig. S7. Experimentally measured VCD and IR spectra for 1-RRS and 1-SSR.

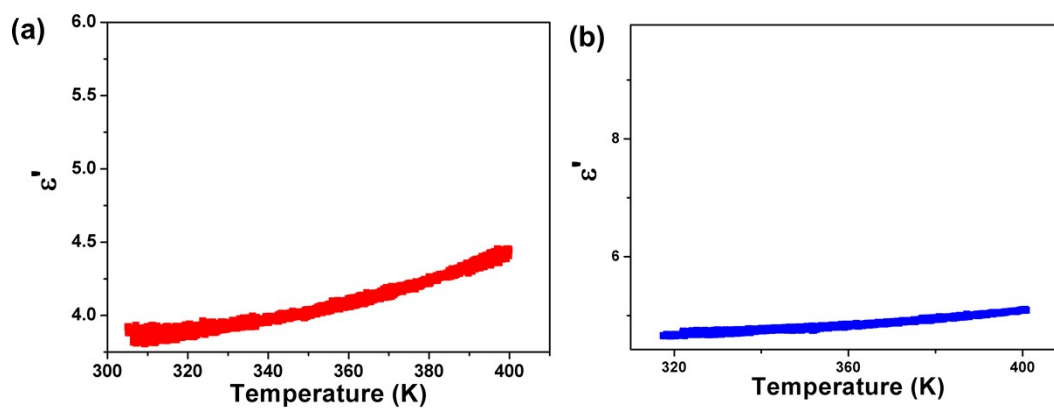


Fig. S8. Dielectric constant measurements for (a) 1-SSR and (b) 1-RRS.

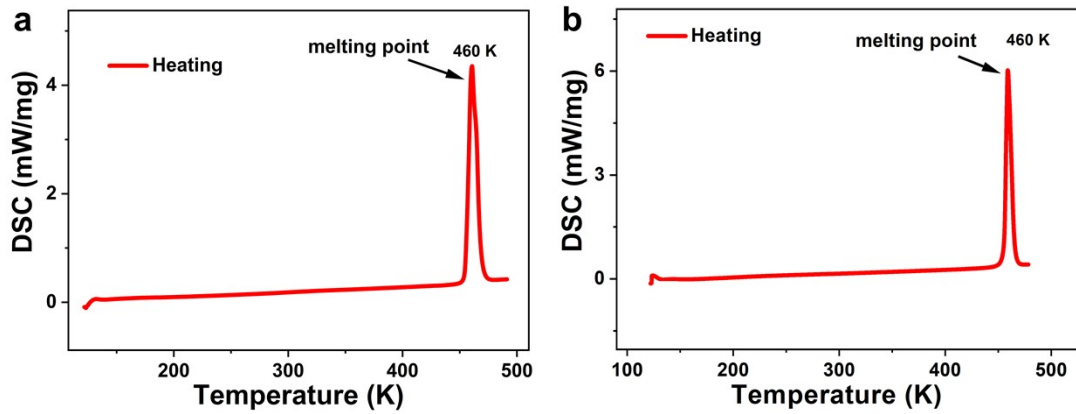


Fig. S9. DSC curves acquired in a heating scan for (a) 1-SSR and (b) 1-RRS.

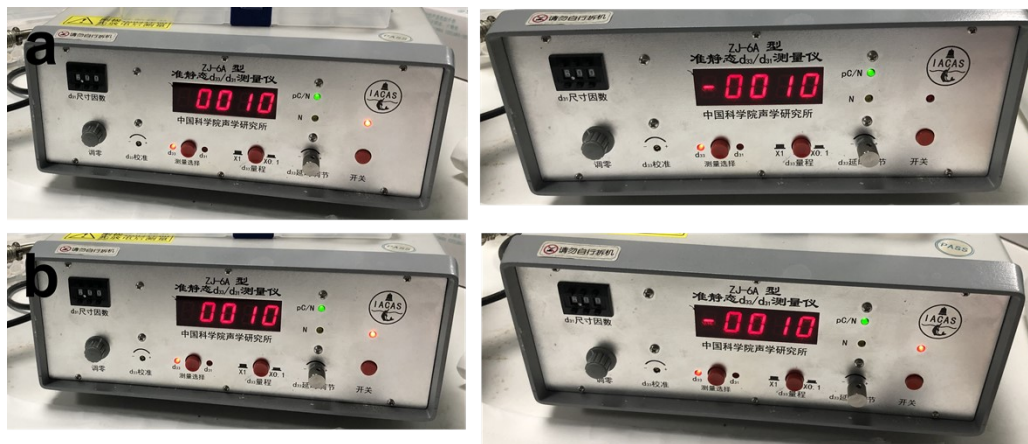


Fig. S10. Raw data of measured piezoelectric constant d_{33} for (a) 1-SSR and (b) 1-RRS, respectively.



Fig. S11. Raw data of measured piezoelectric constant d_{33} for (a) (*R*)-10-camphorsulfonylimine and (b) (*S*)-10-camphorsulfonylimine, respectively.

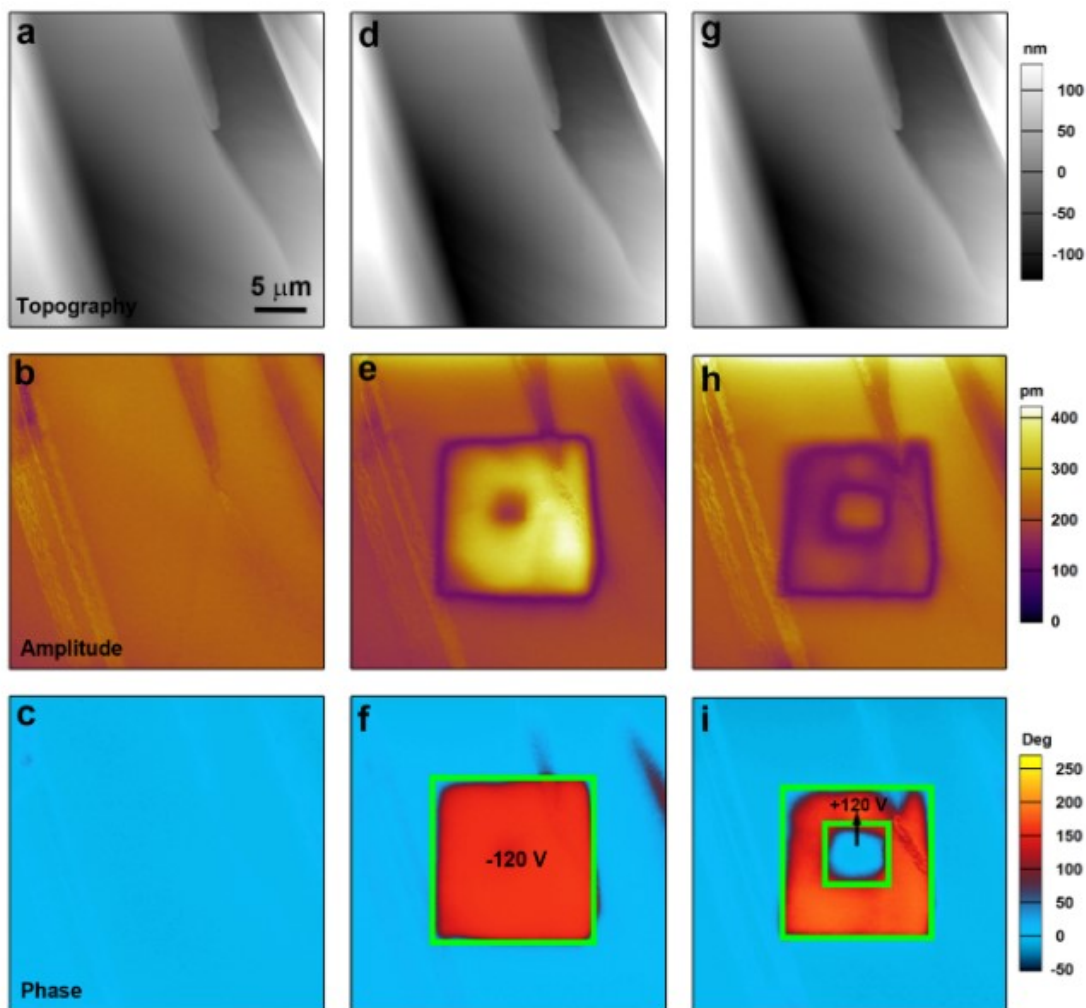


Fig. S12. Morphology of the surface (top) and vertical PFM amplitude (middle) and phase (bottom) images of the 1-RRS thin film at initial state (a-c) and following the polarization switching by voltage of -120 V (d-f) and +120 V (g-i). In the phase images, the red contrast represents upward polarization while the blue contrast represents downward polarization.

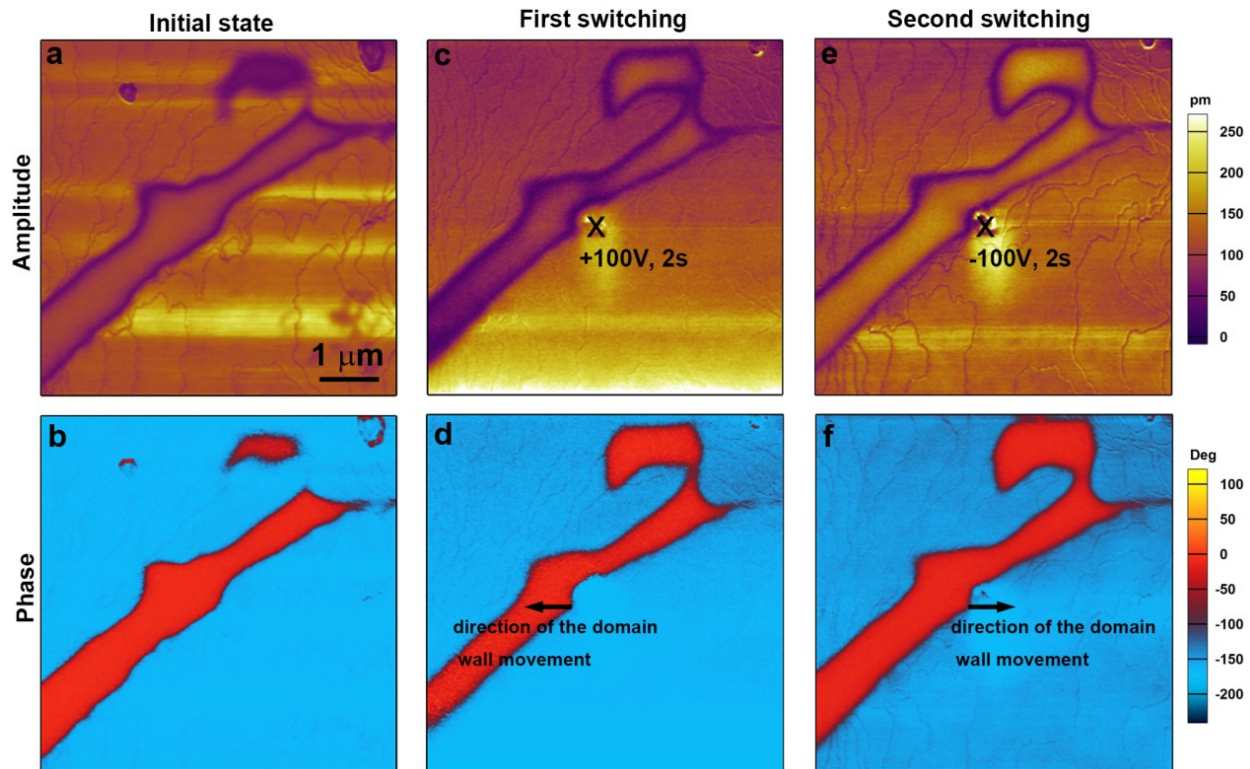


Fig. S13. Evolution of a selected domain detected in the 1-RRS thin film when it is subject to positive and negative electric pulses. (a) PFM amplitude and (b) phase before electric writing. (c) PFM amplitude and (d) phase acquired after subjecting the domain wall to electric pulse of +100 V with 2 s duration. (e) PFM amplitude and (f) phase acquired after subjecting the domain wall to electric pulse of -100 V with 2 s duration. In the phase images, the red contrast represents upward polarization while the blue contrast represents downward polarization.

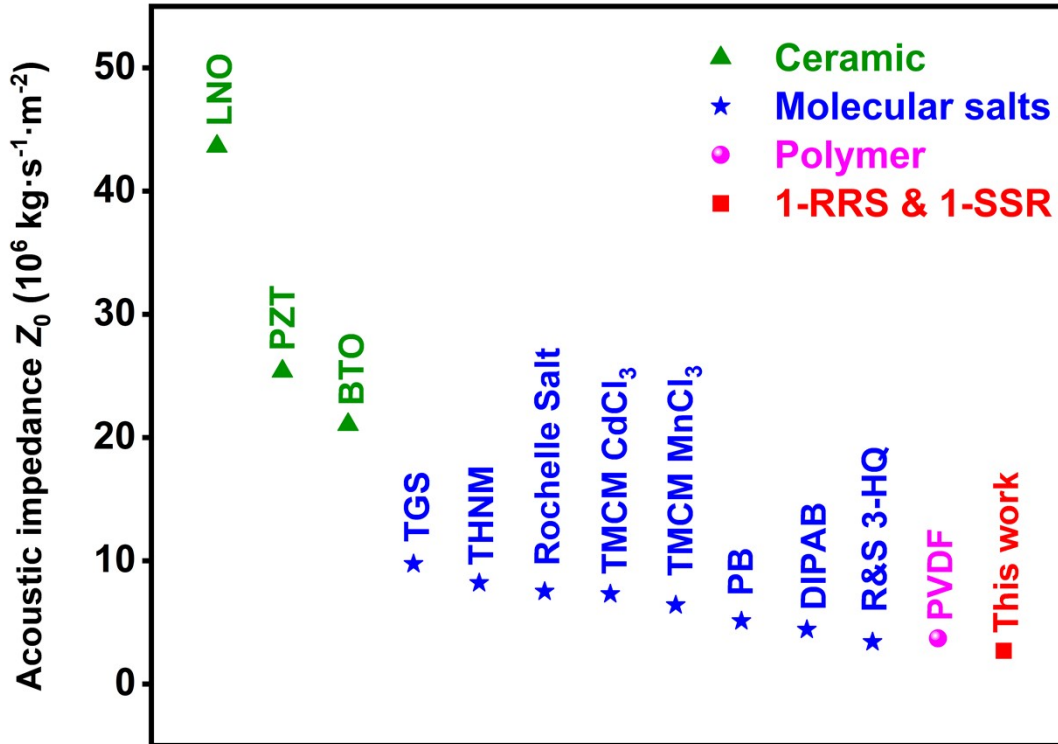


Fig. S14. Acoustic impedance characteristics of 1-SSR and 1-RRS compared with that of ceramic, polymer, and molecular ferroelectrics. LiNbO_3 (LNO), $\text{Pb}(\text{Zr}_{0.52}\text{Ti}_{0.48})\text{O}_3$ (PZT), BaTiO_3 (BTO), Triglycine sulfate (TGS), Tris(hydroxymethyl)nitromethane (THNM),² Trimethylchloromethylammonium cadmium trichloride (TMCMCdCl_3),³ Trimethylchloromethylammonium manganese trichloride (TMCM MnCl_3),³ Diisopropylammonium bromide (DIPAB),⁴ (R and S)-3-hydroxyquinoline (3-HQ),⁵ Poly(vinylidene fluoride) (PVDF).

Table. S1 Crystal data and structure refinements for *I-SSR* and *I-RRS*.

	<i>I-RRS</i>	<i>I-SSR</i>
Temperature	293 K	300 K
Formula	C ₁₃ H ₁₉ N O ₄ S	C ₁₃ H ₁₉ N O ₄ S
Formula weight	285.35	285.35
Crystal system	Monoclinic	Monoclinic
Space group	<i>P2</i> ₁	<i>P2</i> ₁
<i>a</i> (Å)	7.7428(3)	7.7460(2)
<i>b</i> (Å)	7.0274(2)	7.02320(10)
<i>c</i> (Å)	12.3154(4)	12.3152(3)
<i>α</i> (°)	90	90
<i>β</i> (°)	98.214(3)	98.185(2)
<i>γ</i> (°)	90	90
Volume /Å ³	663.23(4)	663.14(3)
<i>Z</i>	2	2
Density/g cm ⁻³	1.429	1.429
<i>R</i> ₁	0.0260	0.0476
<i>wR</i> ₂	0.0740	0.1243
GOF	1.049	1.120

1. B. I. Wilke, A. K. Goodenough, C. C. Bausch, E. N. Cline, M. L. Abrams, E. L. Fayer and D. M. Cermak, *Tetrahedron Letters*, 2010, **51**, 6871-6873.

2. Y. Ai, Y. L. Zeng, W. H. He, X. Q. Huang and Y. Y. Tang, *J Am Chem Soc*, 2020, **142**, 13989-13995.
3. Y.-M. You, W.-Q. Liao, D. Zhao, H.-Y. Ye, Y. Zhang, Q. Zhou, X. Niu, J. Wang, P.-F. Li and D.-W. Fu, *Science*, 2017, **357**, 306-309.
4. D. W. Fu, H. L. Cai, Y. Liu, Q. Ye, W. Zhang, Y. Zhang, X. Y. Chen, G. Giovannetti, M. Capone, J. Li and R. G. Xiong, *Science*, 2013, **339**, 425-428.
5. P. F. Li, W. Q. Liao, Y. Y. Tang, W. Qiao, D. Zhao, Y. Ai, Y. F. Yao and R. G. Xiong, *Proc Natl Acad Sci U S A*, 2019, **116**, 5878-5885.